Molecular Crystals and Liquid Crystals

Publication details, including instructions for authors and subscription information:
http://www.tandfonline.com/loi/gmcl20

Dynamics of the Petal-like Patterns in a Liquid Crystal Light Valve with Rotational Optical Feedback

Tomoyuki Nagaya [a], Shigetoshi Nara [b] & Stefania Residori [c]

[a] Department of Electrical and Electronic Engineering, Oita University, Oita, Japan

[b] Department of Electrical and Electronic Engineering, Okayama University, Okayama, Japan

[c] Institut Non Linéaire de Nice, Université de Nice Sophia-Antipolis, CNRS, Valbonne, France

Version of record first published: 05 Oct 2009

To cite this article: Tomoyuki Nagaya, Shigetoshi Nara & Stefania Residori (2009): Dynamics of the Petal-like Patterns in a Liquid Crystal Light Valve with Rotational Optical Feedback, Molecular Crystals and Liquid Crystals, 511:1, 25/[1495]-35/[1505]

To link to this article: http://dx.doi.org/10.1080/15421400903048495

Mol. Cryst. Liq. Cryst., Vol. 511, pp. 25/[1495]–35/[1505], 2009

ISSN: 1542-1406 print/1563-5287 online
DOI: 10.1080/15421400903048495

Dynamics of the Petal-like Patterns in a Liquid Crystal Light Valve with Rotational Optical Feedback

Tomoyuki Nagaya[1], Shigetoshi Nara[2], and Stefania Residori[3]
[1]Department of Electrical and Electronic Engineering, Oita University, Oita, Japan
[2]Department of Electrical and Electronic Engineering, Okayama University, Okayama, Japan
[3]Institut Non Linéaire de Nice, Université de Nice Sophia-Antipolis, CNRS, Valbonne, France

The bifurcation from the static petal pattern to the fluctuating petal pattern in a liquid crystal light valve with optical rotational feedback is investigated experimentally. At a threshold voltage of the bifurcation, rotationally propagating patches arises on the petals. When increasing the applied voltage, the motion of the patches becomes irregular and the pattern develops into space-time fluctuations. By measuring the time correlation function for the major spatial wave numbers, the characteristic features of the spatiotemporal fluctuations are analyzed in detail.

Keywords: nonlinear dynamics; pattern formation; spatiotemporal instabilities

PACS Numbers: Codes 230.3720,190.3100,190.1450

I. INTRODUCTION

The pattern formation phenomena in extended systems have attracted the attention of researches in various fields. In liquid crystals, a lot of interesting patterns under external fields have been investigated

This work was supported by KAKENHI (Grant-in-Aid for Scientific Research No. 19031026) on Priority Area "Soft Matter Physics" from the Ministry of Education, Culture, Sports, Science and Technology of Japan, by KAKENHI (Grant-in-Aid for Scientific Research No. 18540375) from the Japan Society for the Promotion of Science, and by Toyota Physical and Chemical Research Institute.

Address correspondence to Tomoyuki Nagaya, Department of Electrical and Electronic Engineering, Oita University, 700 Dannoharu, Oita, 870-1192, Japan. E-mail: nagaya@cc.oita-u.ac.jp

intensively [1]. As an example, the electro hydrodynamic convection is one of the oldest and the most studied subject in the field [1]. Recently, the liquid crystal light valve (LCLV) with optical feedback has received a considerable attention [2–10]. From the pioneer work by Akhmanov *et al*. [2,3], many kinds of self-organized patterns have been investigated theoretically and experimentally [2–9].

In the liquid crystal light valve, a nematic liquid crystal and a photoconductor are sandwiched by ITO-coated glass plates. For the reflective type of LCLV, a dielectric mirror is coated on the liquid crystal side of the photoconductor. The liquid crystal side (*reading side*) and the photoconductor side (*writing side*) are optically isolated by the dielectric mirror. Under no illumination on the photoconductor, the liquid crystal molecules are influenced by the anchoring force and remain parallel to the glass plates because most of the applied voltage drops across the photoconductor. On the other hand, when the photoconductor is illuminated, the molecules tilt in accordance with the intensity of the illumination and the applied voltage. If the optical feedback is imposed on the LCLV, the bistable property for the tilt angle of the liquid crystal director arises in several voltage ranges [10]. In such bistable ranges of the voltage, when nonlocal spatial effects are added in the optical feedback, such as rotation of the backward image or diffraction over a free propagation length, self-organized patterns appear [4]. The appearing pattern depends on the type of the feedback and on the control parameters of the experiment, the main ones being the voltage applied to the LCLV, the intensity of the input beam, the initial orientation of the liquid crystal director with respect to the input beam linear polarization, the rotation angle in the feedback loop, the free propagation length.

In the present paper, we focus our attention on the petal patterns observed under the pure-interferential optical feedback (the free propagation length is put equal to zero thanks to a self-imaging system), when spatial rotation is introduced [2,3,6–9]. When the feedback rotation angle Δ is commensurate with 2π, a static pattern consisting of $N = \pi/\Delta$ petals appears at the onset of the bistable voltage ranges. The formation mechanism of the petal pattern was theoretically investigated by Adachihara *et al*. [8]. By increasing the applied voltage V, the static petal pattern becomes unstable at a threshold voltage V_{th} and the pattern start to fluctuate both in space and time. The pattern fluctuations increase with the increase of V. Ramazza *et al*. [9] analyzed the applied voltage dependence of the spatial structure and the activated mode experimentally and theoretically. However, the relaxation frequency of the fluctuations in the fluctuating petal patterns has not been investigated in detail. In the present

paper, we will extract the characteristic features of the fluctuating petal patterns by analyzing the autocorrelation functions in time. By adopting a functional fitting for the autocorrelation function, we will estimate the relaxation frequency. In order to understand space-time chaotic dynamics more precisely, we will measure the time correlation for some spatial modes too. Since the petal pattern appears under the strong effect of the rotational feedback, it is expected that spatial modes relevant to the rotational angle play an important role in the bifurcation. For the case of the pattern consists of N petals, a spatial mode with the wave number N along the azimuthal direction in the polar coordinate and it's harmonic modes correspond to the relevant modes. Then, we will analyze the time correlation for such specific modes and try to identify the most relevant modes able to trigger the bifurcation towards chaotic behavior.

The paper is organized as follows. In Section II we will describe the structure of the LCLV and the experimental setup briefly. In Section III, we will define the physical quantities measured in the image analysis. In Section IV, we will present the experimental results and discuss the characteristic features of the fluctuations. Finally, in the last section, we will summarize the results of the paper.

II. EXPERIMENTAL SETUP

The experimental system to observe the petal patterns under the optical feedback is schematically illustrated in Figure 1. The LCLV

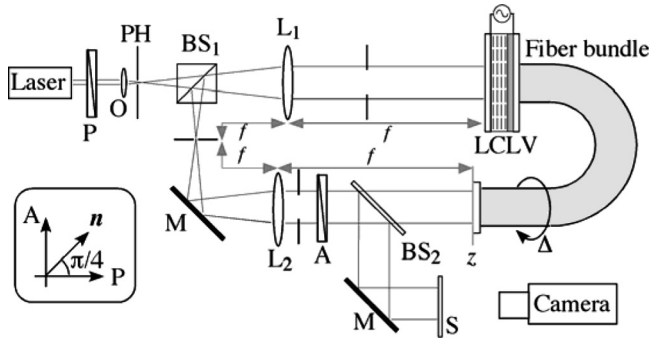

FIGURE 1 Schematic illustration of the optical setup to observe the petal patterns in the LCLV with optical feedback. P: polarizer, A: analyzer, PH: pinhole, O: objective, BS_1, BS_2: beam-splitter, L_1, L_2: lens ($f = 25$ cm), S: screen. The inset indicates the directions of the polarizer P, the director of nematics n, and the analyzer A.

used in the experiment is Hamamatsu PAL-SLM. A laser beam emitted from a He-Ne laser (Neoark model 35) is enlarged and collimated by an objective O, a pinhole PH and a lens $L_1(f = 250\,\mathrm{mm})$. The polarizer selects the horizontal components of the beam. The radius of the diaphragm located in front of the LCLV is 5 mm. In order to exploit the maximum optical anisotropy of the nematic liquid crystal, the director angle is set at $\pi/4$ from the direction of the polarizer P.

The laser beam injected into the nematics is reflected by the dielectric mirror in the LCLV and fed back to the writing side of the LCLV by the lenses L_1, L_2 (of the same focal length, $f = 250\,\mathrm{mm}$), the beam-splitter BS_1 and the fiber bundle. Owing to the optical birefringence of the nematics, the outgoing light from the reading side of the LCLV is elliptically polarized. The phase shift between the ordinary and the extraordinary rays, ϕ, depends on the tilt angle of the nematics. As the analyzer A transmits only the vertical component of the elliptically polarized light, the intensity of the writing light I_w can be written as $I_w = R\{I_0 e^{-\gamma}(1 - \cos\phi)/2\}$ [11], where I_0 represents the intensity of the input laser beam, γ is an effective attenuation coefficient for the optical feedback, and R is the rotational operator introduced by means of the fiber bundle rotation. Thus, the analyzer converts the phase modulations induced by the liquid crystal into intensity modulations in the feedback. The edge of the fiber bundle, which is located at the focal plane of L_2, is mounted on a precision rotating stage. In the present experiment, the feedback image is rotated by $\Delta = \pi/6$, which gives rise to six-fold petal patterns in several voltage ranges.

To observe the feedback image, 5% of the feedback beam is sampled by a beam splitter BS_2. A CCD camera and a frame grabber card (Scion Corporation LG-3) capture successive 300 frames of image with the frame rate 0.04s. The observed images are analyzed by an image processing software (ImageJ) and originally developed programs.

The frequency of the applied voltage is fixed at 1 kHz. The applied voltage, supplied from a synthesizer (NF Corporation WF1944), is varied from 1.87 V to 2.25 V, corresponding to the second bistable regime under the intensity of the incident laser beam $I_0 = 50\,\mu\mathrm{W/cm^2}$. The experimental data here presented were averaged over ten runs of experiments.

III. IMAGE ANALYSIS

Since the petal pattern spreads from the center of rotation, we have analyzed it in the polar coordinates. Then, the intensity of images in the polar coordinates is denoted as $I(r, \theta, t)$. By applying the Fourier

transformation along the azimuthal direction θ, the power spectrum of the space-time image, $P(r,k_\theta,t)=|I(r,k_\theta,t)|^2$, is calculated, where $I(r,k_\theta,t)$ is the Fourier component of $I(r,\theta,t)$ and k_θ is the wave number along the azimuthal direction. The features of the spatial structure of the patterns is evaluated by the averaged power spectra in time, i.e., $P(r,k_\theta)=<P(r,k_\theta,t)>_t$, where $<\cdots>_t$ denotes average in time. To evaluate the degree of fluctuations, the averaged time correlation function, $C(r,t)$, defined as

$$C(r,t)=\left\langle \frac{\langle I(r,\theta,t)I(r,\theta,0)\rangle_t}{\left\langle \left|I(r,\theta,0)^2\right|\right\rangle_t}\right\rangle_\theta,$$

is calculated, where $<\cdots>_\theta$ denotes average in the azimuthal angle. To characterize the fluctuations of the specific azimuthal mode k_θ, furthermore, the time correlation function for the Fourier mode k_θ, defined as

$$C_{k_\theta}(r,t)=\frac{\langle I(r,k_\theta,t)^* I(r,k_\theta,0)\rangle_t}{\left\langle \left|I(r,k_\theta,0)^2\right|\right\rangle_t},$$

is also calculated [12–14], where $*$ means complex conjugate.

IV. RESULTS AND DISCUSION

Instantaneous snapshots of the observed patterns (upper part) and corresponding space-time plots at $r=3$ mm (lower part) are shown in Figure 2. Under the spatial rotation with $\Delta=\pi/6$, the six-fold petal pattern is the basic structure. The six-fold petal pattern appears at $V=1.89$ V. In the voltage regime $1.890\,\mathrm{V}<V<1.999\,\mathrm{V}$, the contrast of the petal pattern increases by the increase of V, which indicates the growth of the mode with $k_\theta=6$, and its multiple harmonic modes. Hereafter we call the mode with $k_\theta=6$ as "*the fundamental mode*". Above $V=1.974$ V, as shown in Figure 2(b), the grey level of the petals changes alternatively along the azimuthal direction. This pattern is also observed in the numerical simulation and named as "*the bicolored petal pattern*" [15]. The appearance of the bicolored petal pattern is caused by the growth of a half subharmonic of the fundamental mode, i.e., $k_\theta=3$.

Above $V=2.023$ V, the static petal pattern becomes unstable and changes to the dynamical pattern. For $V=2.048$ V, as shown in Figure 2(c), regularly propagating patches appear in the petals.

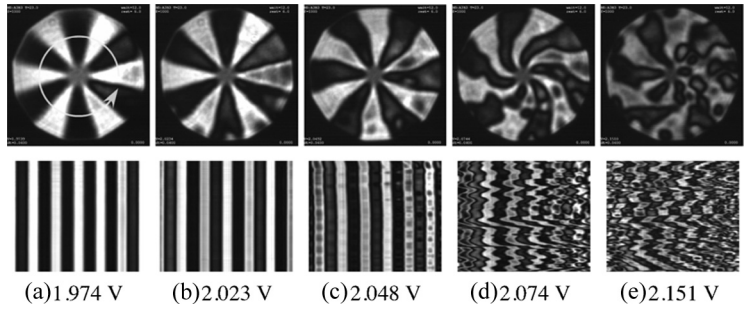

FIGURE 2 Upper part: instantaneous snapshots of the observed patterns for different values of the applied voltage: (a) 1.974, (b) 2.023, (c) 2.048, (d) 2.074, and (e) 2.151 V. The diameter of the pattern is 10 mm. Lower part: corresponding space-time plots; the abscissa and ordinate correspond to the azimuthal angle ($0 < \theta < 2\pi$) at $r = 3.0$ mm and to the time ($0 < t < 12$ s), respectively.

By further increase of V, the propagation of patches becomes irregular (see Figure 2(d)) and then the system develops a fully turbulent state in which reconnection of the petals also occurs (see Figure 2(e)). In this state, the six-fold petal order breaks, except for the center region in which the petal structure is partially sustained by the rotational boundary condition. Above $V = 2.25$ V, the well-developed chaotic pattern disappears because the system exits the bistable region.

The voltage dependence of the power spectrum $P(r, k_\theta)$ at $r = 3$ mm is shown in Figure 3. Since the spatial rotation in the feedback exerts

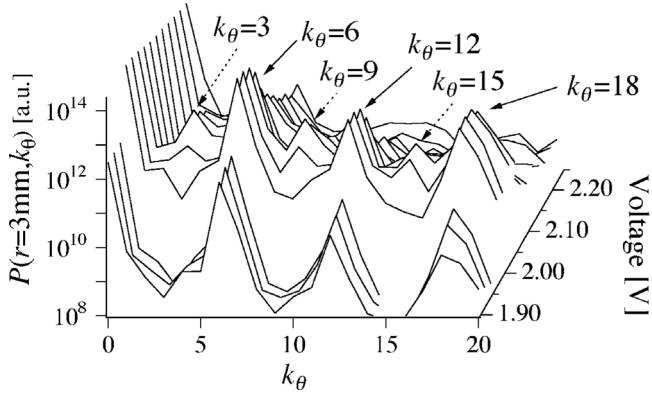

FIGURE 3 Applied voltage dependence of the power spectrum $P(r, k_\theta)$ at $r = 3$ mm.

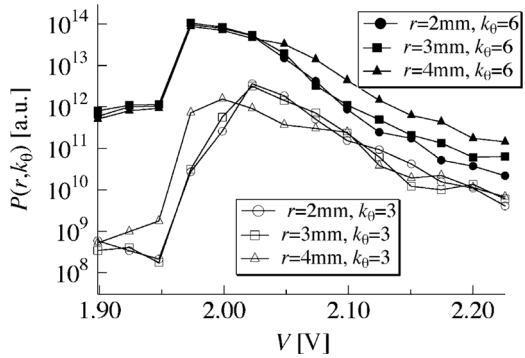

FIGURE 4 Applied voltage dependence of the power of the major modes $k_\theta = 6$ (filled symbols) and 3 (open symbols) at $r = 2$, 3 and 4 mm.

a strong boundary effect on the pattern, $P(r, k_\theta)$ has peaks at the fundamental and its multiple harmonic modes. Therefore, it is expected that these modes play important roles in the bifurcation process. In addition, it should be noticed from Figure 3 that under $1.974\,\mathrm{V} < \mathrm{V} < 2.024\,\mathrm{V}$ the $k_\theta = 3$, 9 and 15 modes indicated by dotted arrows grow rapidly. Then, the applied voltage dependences of the power of two important modes, i.e., $k_\theta = 6$ and 3, at $r = 2$, 3 and 4 mm are plotted in Figure 4. The power of the fundamental mode, $P(r,6)$, has a peak at $V = 1.974\,\mathrm{V}$ and decreases monotonically as the increase of V. Both $P(r,12)$ and $P(r,18)$ show a dependence with

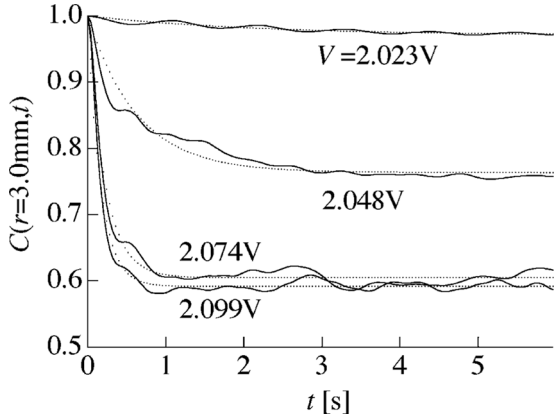

FIGURE 5 Applied voltage dependence of the time correlation function at $r = 3.0$ mm. Solid curves: experimental data. Dotted curves: theoretical fitting.

V similar to that of $P(r, 6)$. Concerning the $k_\theta = 3$ mode, on the other hand, $P(r = 4\,\text{mm}, 3)$ and $P(r = 2{,}3\,\text{mm}, 3)$ have peaks at $V = 1.999\,\text{V}$, and 2.023 V, respectively.

Typical curves of the time correlation function are plotted in Figure 5. To estimate the relaxation time of the fluctuations, $C(r,t)$ is fitted by a simple decay function:

$$C(r,t) = (1 - C_\infty)\exp\left(-\frac{t}{\tau}\right) + C_\infty,$$

where τ is the relaxation time and C_∞ the asymptotic value of the correlation function at $t \to \infty$. The solid and dotted curves in

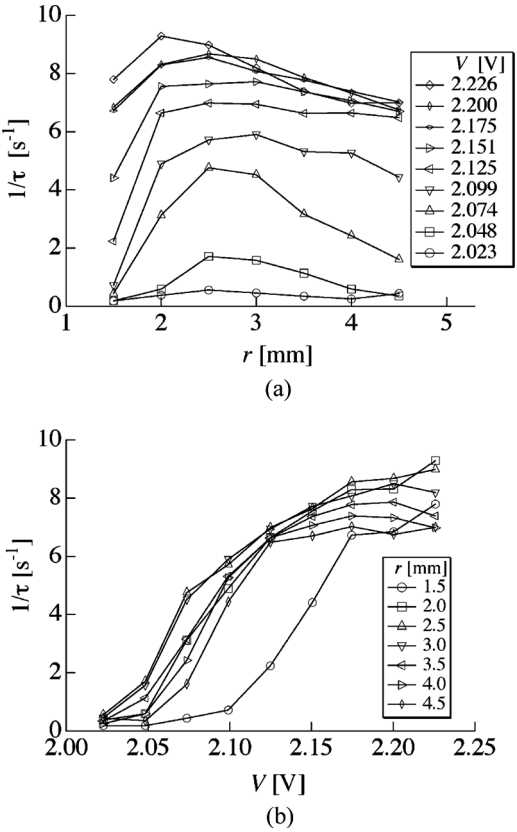

FIGURE 6 Experimentally determined fluctuation relaxation frequency $1/\tau$ as a function of (a) the radial distance r from the center of the pattern and (b) the applied voltage V.

Figure 5 correspond to the experimental data and fitting results, respectively. The radius and the applied voltage dependencies of the relaxation frequency, defined by $1/\tau$, are shown in Figure 6(a) and 6(b), respectively. As shown in Figure 6(a), the fluctuations start around $r \sim 2.5\,\text{mm}$ under $V \sim 2.023\,\text{V}$. Concerning the center part of the image whose radius is less than 1.5 mm, as shown in the circles in Figure 6(b), the fluctuations do not develop so much because the boundary condition imposed by the spatial rotation is very strong in the center part.

The time correlation functions for the fundamental mode $k_\theta = 6$ and its subharmonic mode $k_\theta = 3$ at $r = 3\,\text{mm}$ are shown in Figure 7(a) and

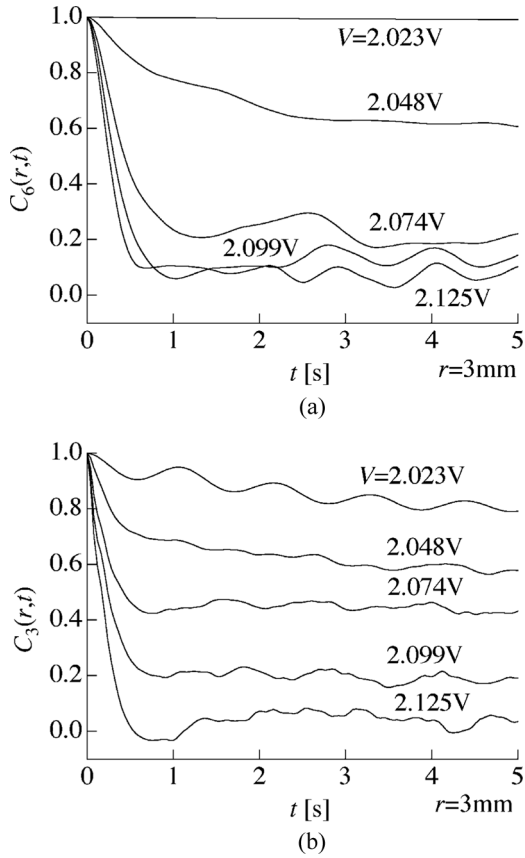

FIGURE 7 Experimentally determined time correlation functions for (a) the $k_\theta = 6$ and (b) the $k_\theta = 3$ mode at the radial distance $r = 3.0\,\text{mm}$ and for different values of the applied voltage.

(b), respectively. Although it is difficult to estimate the relaxation time for each mode from the irregular shape of the correlation functions shown in Figure 7, it is possible to roughly evaluate the characteristic features of the both modes. Under $V = 2.023\,\mathrm{V}$, $C_6(r,t)$ is almost unity, whereas, $C_3(r,t)$ decreases with small oscillations. Generally speaking, the oscillation of the time correlation function is caused by temporal oscillations of the pattern. In the present case, the regularly propagating patches on the petals along the azimuthal direction, shown in the Figure 2(c), may be at the origin of the small oscillations. Therefore, it can be conjectured from these results that the $k_\theta = 3$ is an unstable mode that plays an important role in the bifurcation. When continuing to increase the applied voltage, the regularly propagating motion changes to an irregular one. As a result, the oscillations of $C_3(r,t)$ loses periodicity as shown in Figure 7(b). Above $V = 2.048\,\mathrm{V}$, both $C_6(r,t)$ and $C_3(r,t)$ decrease with irregular oscillations. If we increase the number of averaging in the calculation of $C_{k_\theta}(r,t)$, such irregular oscillations eventually smooth out. In the voltage regime $2.023\,\mathrm{V} < V < 2.074\,\mathrm{V}$, the decrease of $C_6(r,t)$ is faster than that of $C_3(r,t)$. On the other hand, above $V = 2.074\,\mathrm{V}$, there is no remarkable difference in the decay speed of $C_6(r,t)$ and $C_3(r,t)$.

V. CONCLUSION

The spatio-temporal fluctuations of the petal patterns are investigated experimentally in terms of spatial power spectra and time correlation functions. When a spatial rotation with $\Delta = \pi/6$ is introduced in the feedback loop, the six-fold static petal pattern appears at the onset of the bistable voltage regimes. As the applied voltage increases, the amplitude of the six-fold petal pattern develops, which is characterized by an azimuthal spatial wave number $k_\theta = 6$. Slightly below the threshold voltage V_{th} for the bifurcation from the static to the fluctuating pattern, the amplitude of the mode with $k_\theta = 3$, that is the subharmonic mode for the six-fold petal pattern, increases rapidly. As a result the bicolored petal pattern is formed. Just above V_{th}, the patches, that propagate along the azimuthal direction regularly, appear on the petals that may be caused by the fluctuations of the subharmonic mode. Further increase of the applied voltage breaks the six-fold symmetry of the petal pattern, except for the center part, and then the system is lead into a well-developed turbulent regime.

The experimental data obtained in the present work reveal the characteristic behavior of the $k_\theta = 3$ mode. Further theoretical progresses are required to better characterize its role in the bifurcation from the static to the fluctuating six-fold petal patterns.

REFERENCES

[1] Buka, A. & Kramer, L. (1996). *Pattern Formation in Liquid Crystals*, Springer-Verlag: New York.
[2] Akhmanov, S. A., Vorontsov, M. A., & Ivanov, V. Yu. (1988). *J.E.T.P. Lett.*, *47*, 707.
[3] Akhmanov, S. A., Vorontsov, M.A., & Ivanov, V. Yu., Larichev, A. V., & Zheleznykh, N. I. (1992). *J. Opt. Soc. Am. B*, *9*, 78.
[4] Vorontsov, M. A. & Miller, W. B. (1995). *Self-Organization in Optical Systems and Applications in Information Technology*, Springer-Verlag: Berlin.
[5] Neubecker, R., Oppo, G. L., Thuering, B., & Tschudi, T. (1995). *Phys. Rev. A*, *52*, 791.
[6] Arecchi, F. T., Boccaletti, S., Ducci, S., Pampaloni, E., Ramazza, P. L., & Residori, S. (2000). *J. Nonlinear Opt. Phys. Mater.*, *9*, 183.
[7] Residori, S. (2005). *Phys. Rep.*, *416*, 201.
[8] Adachihara, H. & Faid, H. (1993). *J. Opt. Soc. Am. B*, *10*, 1242.
[9] Ramazza, P. L., Residori, S., Pampaloni, E., & Larichev, A. V. (1996). *Phys. Rev. A*, *53*, 400.
[10] Clerc, M. G., Residori, S., & Riera, C. S. (2001). *Phys. Rev., E 63*, 060701 (R).
[11] Khoo, I. C. (1995). *Liquid Crystals: Physical Properties and Nonlinear Optical Phenomena*, Wiley-Interscience Publication: New York.
[12] Oriahra, H., Satou, Y., Nagaya, T., & Ishibashi, Y. (1998). *J. Phys. Soc. Jpn.*, *67*, 2565.
[13] Nagaya, T., Takada, T., & Oriahra, H. (1999). *J. Phys. Soc. Jpn.*, *68*, 3848.
[14] Nagaya, T. & Oriahra, H. (2000). *J. Phys. Soc. Jpn.*, *69*, 3146.
[15] Nagaya, T., Yamamoto, T., Asahara, T., Nara, S., & Residori, S. (2008). *J. Opt. Soc. Am. B*, *25*, 74.